TABLE I.—(*continued*)

No.	R₁	R₂	M.p., °C.ᵃ B.p., °C. (mm. Press.)	Formula	Carbon Calcd.	Carbon Found	Hydrogen Calcd.	Hydrogen Found	Nitrogen Calcd.	Nitrogen Found
				R₃ = —NH(CH₂)₂N(Et)₂						
67	H	H	166–172 (0.16)	C₁₇H₂₆N₂O₂	70.3	70.0	9.0	9.1	9.6	9.6
68	H	CH₃—	170–172 (0.04)	C₁₈H₂₈N₂O₂	71.0	71.1	9.3	9.2	9.2	9.1
69	H	C₂H₅—	156–158 (0.12)	C₁₉H₃₀N₂O₂	...	...	...	...	8.8	9.0
70	C₆H₅CH₂—	H	200–208 (0.08)	C₂₄H₃₂N₂O₂	75.8	75.9	8.5	8.4	7.4	7.4
71	C₆H₅CH₂—	C₂H₅—	204–210 (0.1)	C₂₆H₃₆N₂O₂	76.4	75.9	8.9	8.8	6.9	6.5
				R₃ = —NH(CH₂)₃N(CH₃)₂						
72	H	C₂H₅—	172 (1.0)	C₁₈H₂₈N₂O₂	71.0	71.1	9.3	9.4	...	...
73	p-ClC₆H₄CH₂—	C₂H₅—	226 (0.09)	C₂₅H₃₃ClN₂O₂	70.0	69.9	7.8	7.9	...	...
				R₃ = —NH(CH₂)₃N(C₂H₅)₂						
74	H	H	170–174 (0.12)	C₁₈H₂₈N₂O₂	71.0	71.4	9.3	9.5	9.2	9.0
75	H	CH₃—	184 (0.6)	C₁₉H₃₀N₂O₂	...	...	...	...	8.8	8.4
76	H	C₂H₅—	176–180 (0.18)	C₂₀H₃₂N₂O₂	72.3	72.2	9.7	9.6	8.4	8.5
77	C₆H₅CH₂—	C₂H₅—	224 (0.18)	C₂₇H₃₈N₂O₂	...	...	...	...	6.6	6.6
78	p-ClC₆H₄CH₂—	C₂H₅—	240–250 (0.18)	C₂₇H₃₇ClN₂O₂	70.9	70.9	8.2	8.0	...	...

ᵃ Melting points are not corrected. Recrystallizing solvents: A, hexane; B, ethanol-water; C, ethanol; D, methanol; E, water; F, acetonitrile. ᵇ The esters in some instances were used directly without analyses. Average yield was about 50%. ᶜ Compound is methyl ester. ᵈ Reported Koelsch, C. F., and Scheiderbauer, R. A., *J. Am. Chem. Soc.*, **65**, 2311(1943), m.p. 154–155°. ᵉ Chlorine analysis. ᶠ Derived from *d*-α-methylphenethylamine. ᵍ Picrate of preceding compound. ʰ Reported Kruber, O., and Schmieden, W., *Ber.*, **72B**, 653(1939); m.p. 182°.

of 3.7 Gm. (0.015 mole) of ethyl α-(indan-4-oxy)-butyrate and 15 ml. of diethylaminoethyl amine was heated under reflux for 8 hours, and on distillation gave 3.12 Gm. (66%) of product, b.p. 156–158° at 0.12 mm.

α-(Indan-4-oxy)butyric Acid. (Compound 56.)—A mixture of 22 Gm. (0.088 mole) of ethyl α-(indan-4-oxy)butyrate and 50 ml. of 3 *N* sodium hydroxide was heated under reflux for 2 hours. When cool, and after acidifying with hydrochloric acid, product was extracted with three 100-ml. portions of ether which, on evaporation, gave 18.5 Gm. (95%) of product.

REFERENCES

(1) Shapiro, S. L., Weinberg, K., Bazga, T., and Freedman, L., *J. Am. Chem. Soc.*, **80**, 3729(1958).
(2) Finkelstein, J., and Solodar, W., *ibid.*, **81**, 6508(1959).
(3) Vilax, J. E., British pat. 866,056 (1961).
(4) Garrattini, S., Paoletti, P., and Paoletti, R., "Biochemistry of Lipids," Pergamon Press, Oxford, 1960, pp. 184–193.
(5) Leopold, A. C., "Auxins and Plant Growth," University of California Press, Los Angeles, Calif., 1955.
(6) McMahon, R. E., *J. Med. Pharm. Chem.*, **4**, 67 (1961).
(7) Newman, M., *J. Am. Chem. Soc.*, **72**, 4783(1950).
(8) Shapiro, S. L., Soloway, H., Shapiro, H., and Freedman, L., This Journal, **50**, 973(1961).
(9) Shapiro, S. L., Soloway, H., and Freedman, L., *J. Am. Chem. Soc.*, **80**, 2743(1958).

Melting and Freezing Behavior of Methyl Stearate

By A. P. SIMONELLI† and T. HIGUCHI

Investigations into the mechanism and kinetics of melting and crystallization of the stable form of methyl stearate as followed by changes in its specific volume have shown that: (*a*) the melting behavior was a sensitive function of its immediate history in a manner not associated with polymorphic transitions, (*b*) the thermodynamic equilibrium point was apparently displaced by stirring and that this displacement was proportional to the rate of stirring, (*c*) the rate of crystal growth for the present system was governed largely by the intrinsic rate of two-dimensional nucleation of a crystal plane, and (*d*) the rate of melting was a function of heat transport at higher temperature potentials. The extreme sensitivity of the method used allows the measurement of phase changes where they were of the order of parts per million and enabled the study under very small temperature potentials.

THE RESULTS of an investigation on the rates of melting and freezing are presented. These changes are often of great fundamental importance in altering the appearance of some and the rates of release of other pharmaceutical dosage forms. Although they are extremely common and apparently simple phenomena, relatively little effort seems to have been directed towards the construction of a clear and comprehensive picture of the underlying principles. Past studies in this area have been largely confined to metallic organic or simple organic systems which involve comparatively small entropy changes upon melt-

ing. The present study, on the other hand, has been concerned with the transition rates of systems which are composed of relatively large organic molecules possessing a greater entropy of melting.

The present investigation has dealt specifically with the solidifying and melting rates of methyl stearate as followed by measuring changes in its specific volume. On freezing, the ester exhibits a substantial change in volume corresponding to 30 ml. per mole, and permits the detection of an extremely small phase conversion, changes of the order of 2 p.p.m. being easily followed. These studies include (a) the influence of a thermal gradient on the rate of crystal growth, (b) melting characteristics of methyl stearate crystals formed under a moderate and extremely small temperature gradient, (c) the influence of a thermal gradient on the rate of melting, and (d) the apparent influence of stirring on the crystallization rate.

FACTORS INFLUENCING CRYSTAL GROWTH RATE

The growth of crystals involves several steps among which are transport of material to the surface, plane nucleation, growth of plane nuclei, and abstraction of the heat evolved. The overall net rate, it is evident, is dependent on the relative rates of the individual processes, the rate determining step being the slowest process. During the crystallization process, material from the melt at the interface is deposited upon the crystal and this requires, of necessity, that material must be transported from the bulk of the melt to the surface. The transport of impurity away from the surface of the crystal is also very important. If the rate of crystallization occurs at a slow rate, the concentration of impurity at the interface (molten zone) and the bulk of the melt will not appreciably differ. In the event crystallization is sufficiently rapid, however, the rate of impurity rejection occurring at the rapidly growing interface can overcome the rate of diffusion of impurity away from the interface and cause the impurity concentration at the interface to be appreciably greater than that of the bulk of the melt. This enrichment lowers the melting point and can cause the rate of rapidly growing surfaces to decrease markedly.

The rate of crystal growth is also sensitively dependent on the temperature at the interface. This temperature and the temperature existing in the melt can differ significantly if the heat of fusion which is liberated upon crystallization is not quickly dissipated. The rate of heat transfer from the sample to the bath, dQ/dt, can be estimated for simple geometric forms of sample vessel immersed in a constant temperature bath. It can be shown that the rate is greatly increased by subjecting the sample to stirring.

Even in the event that the rate of mass and heat transfer is infinitely rapid, the rate of crystallization will be limited by the finite rate of formation of the crystalline structure. According to the literature there are four known mechanisms of crystal growth (1–4): upon a rough surface, by a screw dislocation, by two-dimensional nucleation upon a smooth surface, and by three-dimensional nucleation. The rate laws for these mechanisms are

rough surface growth rate $= K_1 \Delta T + A_1$ (Eq. 1)

screw dislocation growth rate $= K_4 \Delta T^2$ (Eq. 2)

2-D nucleation growth rate $=$
$$K_2 \exp \left[-A_2/\Delta T \right] \quad \text{(Eq. 3)}$$

3-D nucleation growth rate $=$
$$K_3 \exp \left[-A_3/\Delta T^2 \right] \quad \text{(Eq. 4)}$$

where ΔT is the temperature potential and K_x and A_x are characteristic constants of the particular system studied. The rate laws derived in the literature, however, have been derived for ideally pure materials, and for this reason the temperature potential can be represented by the temperature difference between the freezing point and the water bath. This assumption tacitly assumes that the equilibrium temperature of the sample is remaining constant as freezing proceeds and is valid only for pure systems.

It would be most difficult to account for the effect of impurity upon the system due to adsorption and occlusion, but the effect of impurity upon the potential can be obtained by considering the thermodynamic equation used in equilibrium dilatometry (5), $N_2 = A_0 \Delta T_f [f/(1-f)]$, where N_2 is equal to the mole fraction of impurity, A_0 is the cryoscopic constant, f is the fraction of the sample that is melted, and ΔT_f is equal to the difference between the freezing point of the mixture, T_m, and the equilibrium temperature of the sample, T_s, at the particular fraction melted, f. The fraction melted can be obtained from a dilatometric curve (5) and is equal to the melting dilation, H, divided by the dilation coefficient, D, of the sample. The dilation coefficient, D, is equal to the total change in height of the mercury in the constant-bore tubing of the dilatometer recorded for complete melting of the sample from the solid state. The melting dilation, H, on the other hand, is equal to the change in height recorded for only a partial melting of the sample from the solid state. The equilibrium temperature of the sample is easily obtained from these relationships, i.e., $T_s = T_m - [N_2/A_0][(1-f)/f]$. The temperature potential of the system, then, is given by the difference between the equilibrium temperature of the sample and the temperature of the water bath, T_b; therefore

$$\Delta T = T_s - T_b = T_m - T_b - \left[\frac{N_2(1-f)}{A_0 f} \right]$$
(Eq. 5)

This equation shows that the temperature potential of an impure system is equal to the temperature potential if it were pure plus a correction factor to account for the effect of the impurity. If Eq. 5 is substituted for the temperature potential, the resulting rate equation can be applied to impure systems

rough surface growth rate $=$
$$K_1 \left(C - \frac{E}{f} \right) + A_1 \quad \text{(Eq. 6)}$$

screw dislocation growth rate $= K_4 \left(C - \dfrac{E}{f} \right)^2$

$$(Eq.\ 7)$$

smooth surface growth rate $=$

$$K_2 \exp \left[\frac{A_2}{C} \left(\frac{f}{f - E/C} \right) \right] \quad (Eq.\ 8)$$

3-D nucleation growth rate $=$

$$K_3 \exp \left[\frac{A_3}{C^2} \left(\frac{f}{f - E/C} \right)^2 \right] \quad (Eq.\ 9)$$

In the above: $C = (T_m - T_b + N_2/A_0)$ and $E = N_2/A_0$.

The above equations predict that the mechanism can be identified by obtaining rate vs. height data at a constant water bath temperature and plotting rate vs. $1/f$, (rate)$^{1/2}$ vs. $1/f$, log (rate) vs. $f/(f - E/C)$, and log (rate) vs. $(f/[f - E/C])^2$, as only one plot should yield a straight line.

EXPERIMENTAL

Apparatus.—The apparatus essentially consisted of a water bath controlled to $\pm 0.001°$ and a dilatometer. The latter apparatus was similar to that previously described (5) with the exception that it was constructed in one piece.

Procedure.—The dilatometer was prepared in the following manner. The sample and stirrer were loaded into a test tube and the open end was sealed to constant-bore tubing as previously described. The end of the dilatometer thus formed was connected by means of a T-tube to an ampul of mercury and to a vacuum pump. After evacuating the system, mercury was introduced by lifting the ampul of mercury until the desired amount of mercury was introduced into the dilatometer. The T-tube was removed and the dilatometer placed into the water bath at a temperature within the melting point range of the mixture to temper the sample overnight. The temperature of the water bath was then slowly dropped to room temperature. The dilatometer was then placed into a high pressure bomb and subjected to a pressure of 3,000 lbs./in.^{2}. This step was necessary in order to eliminate void space which otherwise obscures the data. Finally the dilatometer was placed into the water bath. To investigate transition rates the temperature of the water bath was changed sharply and the mercury height read with a micrometer microscope at intervals of 1 to 5 minutes. From an equilibrium melting curve the readings were converted to fractions of the sample melted, f. The rates as a function of the fraction melted were obtained from the slopes of the fraction melted vs. time plots of this data. In another method the temperature of the water bath was varied by increments. Fraction melted-time readings were recorded at each temperature setting for short intervals in order to limit the change in the fraction of the sample melted. By alternately applying a freezing and melting potential, the variation of the fraction melted was held to a minimum. In this way the fraction of the sample melted was approximately constant, and the slopes of the various fraction melted-time plots at each temperature setting yielded the rate at the particular temperature of the water bath. This method allowed the simultaneous study of melting and freezing as a function of the temperature.

The first method, which maintained a constant water bath temperature and a varying fraction melted, was preferred as the water bath temperature was rigidly controlled and the fraction melted can be measured very accurately. The second method, on the other hand, requires a constant fraction melted and a varying temperature; yet the fraction melted must be allowed to vary in order to obtain a rate; in addition, heat transfer and mercury expansion can affect the results if the fraction melted-time readings are taken for too short a time. This method, however, enjoys the advantage of requiring much less time to complete a rate study.

Sources of Materials.—Three lots of methyl stearate were used in this study. Eastman Kodak reagent grade methyl stearate was recrystallized several times from methanol. This methyl stearate is obtained by fractional distillation of natural products, but a gas chromatogram indicated that it was contaminated by methyl palmitate. The melting point of this sample was 38.33° and it was estimated from a dilatometric melting curve that it contained 0.065 mole fraction of impurity. Methyl stearate was also obtained by the reduction of methyl oleate. A gas chromatogram showed that the sample obtained in this manner was relatively free from methyl palmitate. The melting point of this sample was 38.60° and it was estimated that it contained 0.042 mole fraction of impurity. Recrystallization from methanol three times and then from Skelley C three times increased the melting point to 39.05° and decreased the impurity to 0.004 mole fraction.

RESULTS AND DISCUSSION

Establishment of Mechanism of Crystal Growth.—Dilatometric investigations on the rate of crystal growth as a function of the degree of supercooling were carried out on the three relatively pure lots of methyl stearate. Essentially the method employed was based on continual determination of the fraction melted of a partly solidified and slowly freezing sample of the lipid. The measurements are reported in terms of the fraction of the sample melted obtained by measuring the heights of the mercury column as observed in the dilatometer, the total height change for complete freezing from the liquid state being of the order of 40 cm. The sample was brought to near equilibrium at such temperature 38.75° that approximately 75% was in the liquid state. The temperature was then dropped sharply by a few tenths of a degree and the capillary height of the dilatometer was observed from time to time. A plot of the fraction melted vs. time was prepared and the rates at various degrees of crystallization were recorded.

In Figs. 1 and 2 these rates of crystal growth have been plotted as several functions of f, the melting dilation expressed as fractions of the sample melted. It is evident that according to preceding discussions, the rates appear to obey Eq. 8 or 9, based on the two- or three-dimensional nucleation as the rate determining step.

Since the above run was determined on a system largely melted, a run at a lower degree of melting was carried out to differentiate between these two
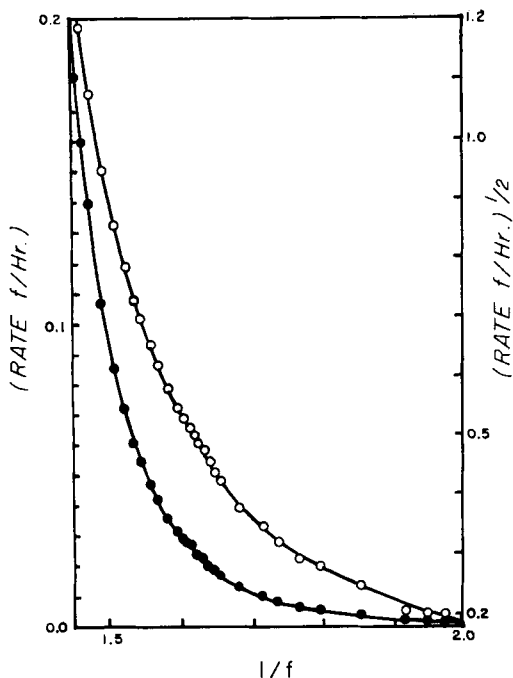
Fig. 1.—The rate data of the same experiment plotted according to Eqs. 6 and 7. ●, rate *vs.* 1/*f*. ○, (rate)$^{1/2}$ *vs.* 1/*f*.
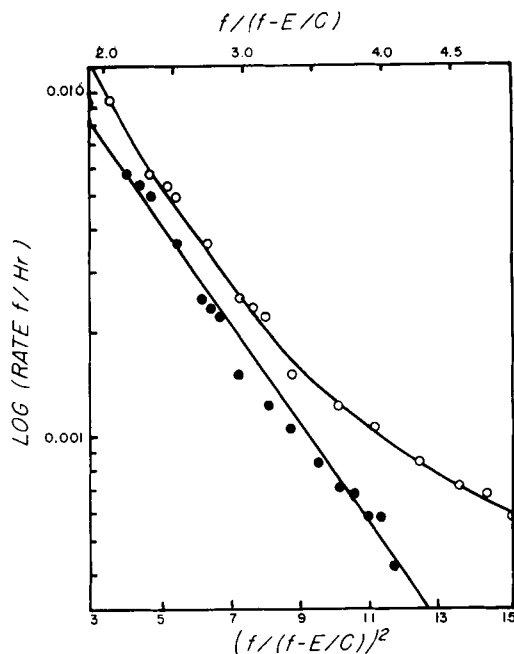

Fig. 3.—The rate data of the same experiment plotted according to Eqs. 8 and 9. This experiment was conducted at a relatively low degree of sample melting. ●, log(rate) *vs.* [*f*/(*f* — *E*/*C*)]. ○, log(rate) *vs.* [*f*/(*f* — *E*/*C*)]^2.

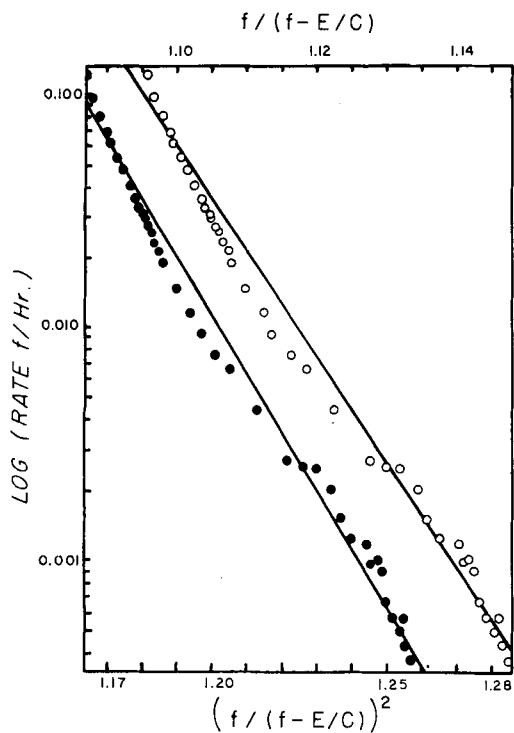
Fig. 2.—The rate data of the same experiment as Fig. 1 plotted according to Eqs. 8 and 9. ●, log(rate) *vs.* [*f*/(*f* — *E*/*C*)]. ○, log(rate) *vs.* [*f*/(*f* — *E*/*C*)]^2.

mechanisms. The results are shown by Fig. 3 and indicate that the crystal growth is governed largely by the intrinsic rate of formation of crystal planes.

To substantiate this the rate of phase transformation under fixed conditions except for temperature was determined as a function of temperature. In this method the equilibrium temperature of the sample at its observed height was first obtained from its dilatometric melting curve (5). A freezing potential was then applied to the system by sharply dropping the water bath temperature, the fraction melted-time readings being taken, however, only for a sufficient time to establish the rate. The sample then was remelted until the fraction of the sample melted had increased to its initial point and then the temperature of the water bath was again sharply dropped to another temperature. In this manner the rates of crystallization were obtained directly as a function of the supercooling, $T_s - T_b$. Figure 4 shows that a plot thus determined of the log (rate) *vs.* 1/ΔT is a straight line verifying the previous results that the rate law which governs this system is that the rate = $K_2 \exp (-A_2/\Delta T)$. This strongly suggests that the rate determining process for crystal growth in this system was nucleation of crystal planes, the extension of the nucleus to the edges being relatively rapid. Figures 1 to 4 were determined using the sample containing 0.004 mole fraction of impurity. All samples, however, displayed the same behavior.

Melting Characteristics of Methyl Stearate Crystals Formed under a Moderate and Extremely Small Temperature Gradient.—The melting behavior of methyl stearate was found to be a rather sensitive function of its immediate history in a
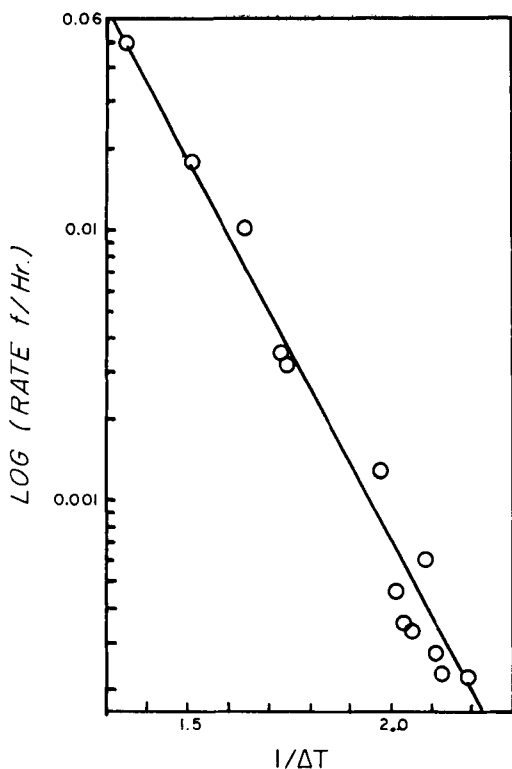
Fig. 4.—The log(rate) as a function of $1/\Delta T$.

HOURS

Fig. 5.—The effect of past history upon "after-melting" contraction. Curve A, initial run where $T°$ was changed from 37.08 to 37.50°. Curve B, rerun after freezing the sample very slowly with the aid of stirring where $T°$ was changed from 37.08 to 37.50°. Curve C, third run after freezing the sample very rapidly without any stirring where $T°$ was changed from 36.76 to 37.29°.

manner not associated with polymorphic transitions. When the system was exposed to a melting potential, the sample was observed to contract after initially expanding for a period of time. Although the rate of contraction decreased with time, the recovery process persisted as long as 7 days without stopping. This peculiar behavior will be referred to as "after-melting" contraction, and is illustrated by curve A of Fig. 5 which shows the fraction of the sample melted readings recorded after applying a melting potential to the system.

This phenomenon can be possibly rationalized as being due to imperfections in the crystal structure induced by excessive growth rates. The crystal eliminates these stresses by overmelting and then refreezing. Impurity can exert the same effect if its distribution is not thermodynamically stable within the solid sample as it will redistribute itself during melting.

If either of the above is responsible for "after-melting" contraction, then, crystallizing the sample under equilibrium conditions should tend to diminish its effect. The sample was melted and then solidified using a small temperature potential and with the aid of stirring. The results of the rerun are shown by curve B in Fig. 5. Comparison with A shows that "after-melting" contraction was significantly eliminated. To check this further the sample was again melted and solidified using a large temperature potential without the aid of stirring. Curve C in Fig. 5 shows that the effect of these harsh conditions greatly increased "after-melting" contraction and seems to indicate that the above explanations may be true. Although samples of
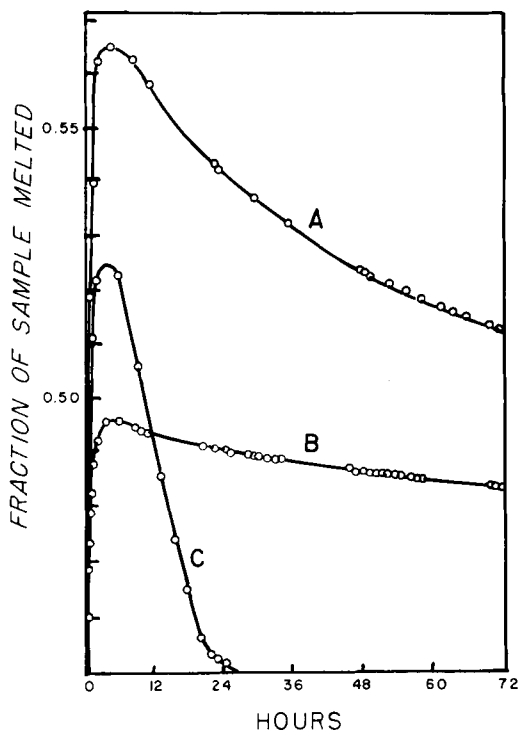
varying purity were used, the effect always appeared. This seems to indicate that "after-melting" contraction may be largely due to the presence of crystal imperfections.

Influence of a Thermal Gradient on the Rate of Melting.—The mechanism of melting was investigated, and it was found that a plot of the melting rate *vs.* the reciprocal fraction melted yielded a straight line. Some of the runs, however, revealed a break in the curve between the rates of 3,000 to 5,000 mg./min. This suggests that the determining factor at high melting rates differs from that which is operative at the lower rates. This is illustrated by Fig. 6.

According to Eqs. 1 and 6, a plot of the rate *vs.* the reciprocal fraction melted will be straight in the event the rate is first order with respect to the temperature potential. In this case, either melting from a rough surface is occurring or heat transfer is the governing factor. For this study the rate of heat transfer from the bath to the sample, dQ/dt, in the presence of stirring can be calculated from

$$\frac{dQ}{dt} = \frac{K_g A \Delta T}{n} \text{ cal./sec.} \qquad \text{(Eq. 10)}$$

where n is the thickness of glass in dilatometer, K_g is the heat conductivity of glass, A is the area of the glass, and ΔT is the temperature potential. The theoretical rate of heat transfer calculated from
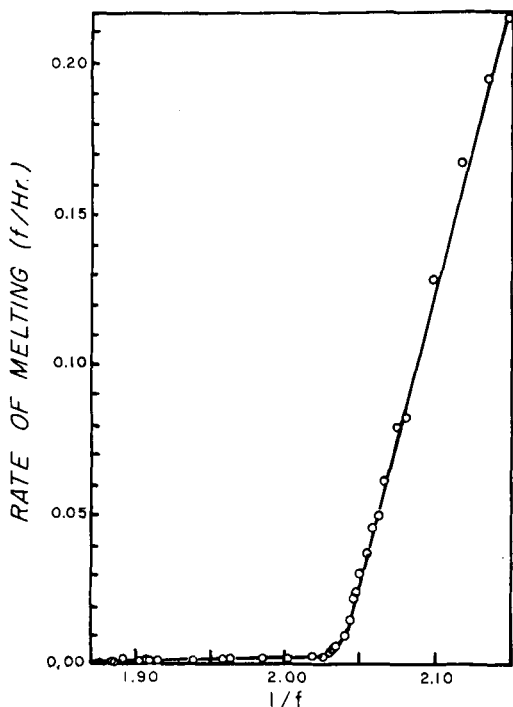
Fig. 6.—The rate of melting as a function of the reciprocal fraction melted.

Fig. 7.—The effect of stirring upon the fraction of the sample melted *vs.* time curve.

Fig. 8.—The rate of expansion as a function of the rate of stirring. O, the observed rate; ●, the net rate (the observed rates with stirring less the observed rate of the unstirred sample).

the above is approximately 100 cal./°C./min. If the governing rate is the rate of heat transfer, then Eq. 10 predicts that the value of K_1 in Eq. 1 will be equal to $(K_gA)/n$ or 100 cal./°C./min. At the same time, Eq. 6 predicts that the value of K_1 can be calculated from the slope of the rate *vs.* reciprocal fraction melted curve as the slope is equal to $(K_1N_2)/A_0$. The values of K_1 which were calculated from the beginning slopes of a few runs seem to indicate that heat transfer is the governing factor at fast rates of melting as the values of K_1 were approximately 100 cal./min.

The slope of the straight line after the break varied greatly, indicating that the slope may depend upon experimental conditions. A possible cause may be the effect of "after-melting" contraction, which varies in degree from one run to another depending on the past history. It may also be possible that the rate is not proportional to ΔT in this region, but may be proportional to some other function of ΔT.

Since the first part of the curve was not determined by the rate of melting, only the slower rates can be used to determine the rate law; at low potentials, however, the rates become very sensitive to the effects of heat transfer, "after-melting" contraction, temperature, surface area, and other experimental conditions. Since these variables complicate the rate data, the mechanism of melting was not investigated any further.

Apparent Influence of Stirring on the Crystallization Rate.—An unstirred sample which was solidifying at a slow rate was observed to undergo the reverse process when stirring was initiated and refreeze when stirring was stopped. A system
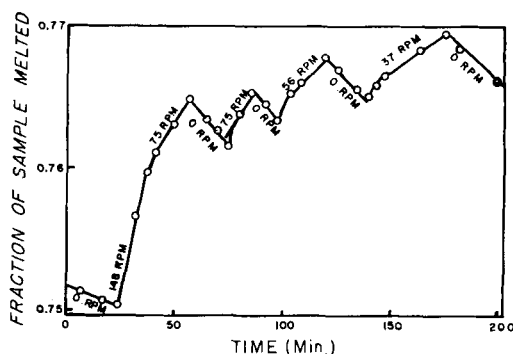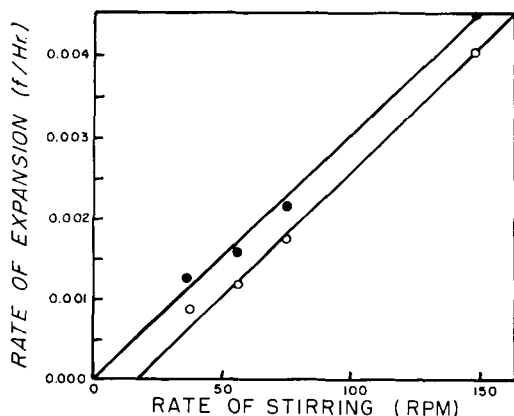
of pulleys which allowed the rate of stirring to be varied over a wide range was utilized to study this peculiar behavior further. A typical plot of the height *vs.* time with a varying rate of stirring is shown by Fig. 7. The slopes of the curve at the various rates of stirring were obtained, and the rates were plotted *vs.* the rate of stirring expressed as revolutions per minute (r.p.m.). The plot of the observed and net rates are shown in Fig. 8, revealing straight line relationships. The exact reason for this behavior has not been established.

Discussion.—Previous studies involved measurements of the linear rate upon one plane of the crystal, maintained a constant surface area, utilized highly purified substances, and relied upon diffusion for all transport processes. This study, however, utilized samples whose purity varied over a wide range and involved dilatometric measurements of the combined growth of all planes of a variable number of crystals. Most important, however, the conditions of this study more closely resemble those of industry (free growth with stirring) which permit the results to be more readily applied to industrial systems.

The study of the rates of phase transitions can yield useful information which can be utilized to advantage in the production and storage processes

by the pharmaceutical industry. Many of the substances used in the formulation of medicinals are polymorphic and frequently exhibit melting points, solubilities, pharmacological activities, and other important properties which differ markedly from each other; as a result, the conversion of one form to another upon aging presents an important problem, as it can often curtail the shelf life of products.

REFERENCES

(1) Wilson, H. A., *Phil. Mag.*, **50**, 238(1900).
(2) Hillig, W. B., and Turnbull, D. J., *J. Chem. Phys.*, **24**, 914(1956).
(3) Volmer, M., and Marder, M., *Z. physik. Chem. Leipzig A.*, **154**, 97(1931).
(4) Frenkel, J., "Kinetic Theory of Liquids," Oxford University Press, 1946, p. 413.
(5) Simonelli, A. P., and Higuchi, T., THIS JOURNAL, **50**, 861(1961).

Notes

Chemical Effect of High Level Gamma Irradiation on Blood Glucose *in Vitro*

By LINDA KAY RAMES† and HAROLD S. BAILEY

Furan-2,5-dicarboxylic acid is one of the decomposition products of blood glucose subjected to high energy gamma irradiation.

THE EFFECT of ionizing radiation on materials of biological interest is important to our understanding of radiation hygiene. Pioneering studies have been made on the changes produced in amino acids, proteins, carbohydrates, and other biochemicals upon bombardment with nuclear radiation.

Changes in aqueous solutions of biochemicals upon irradiation are complex. Due to free radical formation, a large quantity of hydrogen is formed upon irradiation of water containing traces of halides. Also, dissolved oxygen in irradiated water will react with (H) radicals present to form the free radical (HO_2). Therefore, oxidizable or reducible solutes present in an irradiated aqueous medium may be readily oxidized or reduced.

Because of its importance to living organisms, we have been interested in the effect of ionizing radiation on blood glucose.

It is possible that the effect of irradiation of blood glucose and other blood constituents may provide an insight into the mechanism of radiation sickness. Since blood acts as a transportation agent for the body and as a solvent for so many complex compounds, it could be the source or carrier of toxic decomposition products resulting from irradiation.

Radiation effects on blood glucose have been noted both *in vitro* and *in vivo* (1–4). Irradiation of both dogs and rats has resulted in the development of hypoglycemia.

One could expect that the effects of ionizing radiation on blood might produce several by-products from blood glucose since blood would yield many other ions and radicals besides those of water upon

irradiation. These other substances may alter the process of decomposition or react quickly with the products.

Previous research by us indicated that furan-2,5-dicarboxylic acid might be one of the irradiation decomposition products of glucose solutions. The objective of this study, therefore, was to show whether furan-2,5-dicarboxylic acid is produced upon irradiation of blood.

EXPERIMENTAL

Irradiation of Blood Plasma.—Rabbit blood plasma was chosen as the medium in which the effects of gamma radiation on blood glucose would be studied. Heparinized blood was centrifuged, the plasma decanted, and kept under refrigeration. Some hemolysis occurred.

A total of 9.01 mg. of radioactive glucose randomly-labeled with carbon[14] was added to 8 ml. of the blood plasma contained in a small beaker. The specific activity of the radioglucose was 1.0 mc. per mmole, and a total activity of 50 μc. was present. After solution was evident, the blood plasma was poured into a half-ounce prescription bottle, and the beaker was rinsed twice with approximately 4-ml. portions of blood plasma, the rinsing combined with the original solution in the bottle.

For irradiation, the bottle containing the labeled blood plasma was fastened to a pegboard constructed in such a manner that the cobalt[60] irradiation source could be positioned at a known distance by remote control. The source was placed exactly 3 inches from the bottle.

The Co[60] source had a gamma ray activity of 103.6 curies. At a distance of 3 inches the blood plasma received an approximate dose of 23,760 roentgens per hour or a total of approximately 1,200,000 roentgens in the 50.5 hours of irradiation.

Radiochemical Analysis by the Carrier Technique.—A 100-mg. portion of synthesized furan-2,5-dicarboxylic acid was added to the irradiated plasma. The carrier furan-2,5-dicarboxylic acid was then solated from the irradiated system by the following process.